

Rotational Symmetry Breaking in the Hidden-Order Phase of URu₂Si₂

R. Okazaki^{1,*}, T. Shibauchi^{1,†}, H. J. Shi¹, Y. Haga², T. D. Matsuda²,

E. Yamamoto², Y. Onuki^{2,3}, H. Ikeda¹, and Y. Matsuda¹

¹Department of Physics, Kyoto University, Kyoto 606-8502, Japan

²Advanced Science Research Center, Japan Atomic Energy Agency, Tokai 319-1195, Japan

³Graduate School of Science, Osaka University, Toyonaka, Osaka 560-0043, Japan

*Present address: Department of Physics, Nagoya University, Nagoya 464-8602, Japan

†To whom correspondence should be addressed. E-mail: shibauchi@scphys.kyoto-u.ac.jp

(Dated: published January 28, 2011)

A second-order phase transition is characterized by spontaneous symmetry breaking. The nature of the broken symmetry in the so-called “hidden order” phase transition in the heavy fermion compound URu₂Si₂, at transition temperature $T_h = 17.5$ K, has posed a long-standing mystery. We report the emergence of an in-plane anisotropy of the magnetic susceptibility below T_h , which breaks the four-fold rotational symmetry of the tetragonal URu₂Si₂. Two-fold oscillations in the magnetic torque under in-plane field rotation were sensitively detected in small pure crystals. Our findings suggest that the hidden-order phase is an electronic “nematic” phase, a translationally invariant metallic phase with spontaneous breaking of rotational symmetry.

A second-order phase transition generally causes a change in symmetry, such as rotational, gauge, or time-reversal symmetry. An order parameter can then be introduced to describe the low-temperature ordered phase with a reduced symmetry. The heavy-fermion compound URu₂Si₂ undergoes a second-order phase transition at $T_h = 17.5$ K, which is accompanied by large anomalies in thermodynamic and transport properties [1–3]. Because the nature of the associated order parameter has not been elucidated, the low-temperature phase is referred to as the hidden-order phase. It is characterized by several remarkable features. No structural phase transition is observed at T_h . A tiny magnetic moment appears ($M_0 \sim 0.03\mu_B$, where μ_B is the Bohr magneton) below T_h [4], but it is far too small to explain the large entropy released during the transition and seems to have an extrinsic origin [5–7]. An electronic excitation gap is formed on a large portion of the Fermi surface and most of the carriers ($\sim 90\%$) disappear [8–10]; a gap is also formed in the incommensurate magnetic excitation spectrum [11].

The nature of the hidden order cannot be determined without understanding which symmetry is being broken. Several microscopic models, including multipole ordering [12–16], spin-density wave formation [17–19], orbital currents [20], and helicity order [21], have been proposed. However, despite intensive experimental and theoretical studies, this remains an open question.

The measurement of the magnetic torque $\tau = \mu_0 \mathbf{M} \mathbf{V} \times \mathbf{H}$ has a high sensitivity for detecting magnetic anisotropy. Here V is the sample volume, \mathbf{M} is the induced magnetization, \mathbf{H} is the magnetic field, and μ_0 is the permeability of vacuum. In particular, torque measurements performed for a range of directions of \mathbf{H} spanning the tetragonal ab plane in URu₂Si₂ provide a stringent test of whether the hidden-order parameter breaks the crystal four-fold symmetry. In such a geometry, τ

is a periodic function of double the azimuthal angle ϕ measured from the a axis:

$$\tau_{2\phi} = \frac{1}{2} \mu_0 H^2 V [(\chi_{aa} - \chi_{bb}) \sin 2\phi - 2\chi_{ab} \cos 2\phi], \quad (1)$$

where the susceptibility tensor χ_{ij} is given by $M_i = \sum_j \chi_{ij} H_j$ (Fig. 1). In a system holding tetragonal symmetry, $\tau_{2\phi}$ should be zero because $\chi_{aa} = \chi_{bb}$ and $\chi_{ab} = 0$. Finite values of $\tau_{2\phi}$ may appear if a new electronic or magnetic state emerges that breaks the tetragonal symmetry. In such a case, rotational symmetry breaking is revealed by $\chi_{aa} \neq \chi_{bb}$ or $\chi_{ab} \neq 0$ depending on the orthorhombicity direction.

Figure 2A depicts the torque measured in field \mathbf{H} , the orientation of which is varied within a plane that includes the c axis (Fig. 2A, inset). Both below and above T_h , the curves are perfectly sinusoidal and can be fitted with $\tau(T, H, \theta) = A_{2\theta}(T, H) \sin 2\theta$, where A is the amplitude,

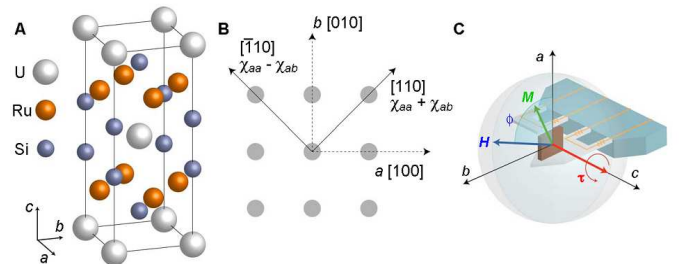


FIG. 1. (A) The tetragonal crystal structure of URu₂Si₂. (B) U atom arrangement in the ab plane. The relevant axes and the susceptibility components for the $\chi_{aa} = \chi_{bb}$ case are also shown. (C) Schematics of in-plane ϕ -scan measurements. The magnetic field \mathbf{H} was applied in the ab plane with high alignment precision (within 0.02°).

θ is the polar angle, and T is absolute temperature. In our carefully selected crystals [22], no hysteresis is observed, indicating no detectable ferromagnetic impurities (the hysteresis component is less than 0.01% of the total torque). In this geometry, the difference $\Delta\chi_{ca}$ between the c -axis and in-plane susceptibilities yields a two-fold oscillation term $\tau_{2\theta}(\theta, T, H)$ with respect to θ rotation,

$$\tau_{2\theta} = \frac{1}{2}\mu_0 H^2 V \Delta\chi_{ca} \sin 2\theta. \quad (2)$$

The H -linear dependence of $A_{2\theta}(H, T)/H$ with a negligible y -intercept (Fig. 2B) indicates a field-independent magnetic susceptibility—that is, a purely paramagnetic response. This also reinforces the absence of ferromagnetic impurities. To check the consistency of the data, we also measured the susceptibility of a different single crystal of URu₂Si₂ in the same batch by means of a superconducting quantum interference device (SQUID) magnetometer (Fig. 2C). The amplitudes of $\Delta\chi_{ca}$ obtained in the two types of measurements coincide in both the hidden-order and paramagnetic states.

Having established the evidence of the purely paramagnetic response in our single crystals, we now consider the in-plane torque measured in \mathbf{H} rotating within the ab plane. To exclude two-fold oscillations appearing as a result of misalignment, \mathbf{H} is precisely applied in the ab plane within an error of less than 0.02° by controlling two superconducting magnets and a rotating stage [22] (Fig. 1C). Shown in Fig. 2, D to H, is the temperature evolution of the torque $\tau(\phi)$ at 4 T in the hidden-order phase. All torque curves are perfectly reversible with respect to the field rotation direction; $\tau(\phi)$ can be decomposed as $\tau = \tau_{2\phi} + \tau_{4\phi} + \tau_{6\phi} + \dots$, where $\tau_{2n\phi} = A_{2n\phi} \sin 2n(\phi - \phi_0)$ is a term with $2n$ -fold symmetry with $n = 1, 2, \dots$. In the middle and lower panels of Fig. 2, D to H, the two-fold and four-fold components obtained from the Fourier analysis are displayed.

Our results show that the two-fold oscillation is distinctly observed in the hidden-order state, whereas it is absent in the paramagnetic phase at $T = 18$ K slightly above T_h (middle panels of Fig. 2, D to H). Indeed, the torque curves shown in the upper panels become asymmetric with respect to 90° rotations below T_h . We note that the observed four-fold oscillations $\tau_{4\phi}$ (and higher-order terms) arise primarily from the nonlinear susceptibilities [23]. The presence of the two-fold oscillation, which follows the functional form $\tau_{2\phi} = A_{2\phi} \cos 2\phi$, clearly demonstrates that $\chi_{ab} \neq 0$, whereas $\chi_{aa} = \chi_{bb}$. Figure 3A depicts the temperature dependence of $|A_{2\phi}|/V$, which indicates sizable in-plane anisotropy $2\chi_{ab}/\chi_{aa}$ at low temperatures. The two-fold amplitude becomes nonzero precisely at $T_h = 17.5$ K (Fig. 3A, inset). This result, together with the absence of hysteresis in the torque curves, rules out the possibility that very tiny ferromagnetic impurities are the origin of the two-fold symmetry [22]. Moreover, $|A_{2\phi}|$ grows

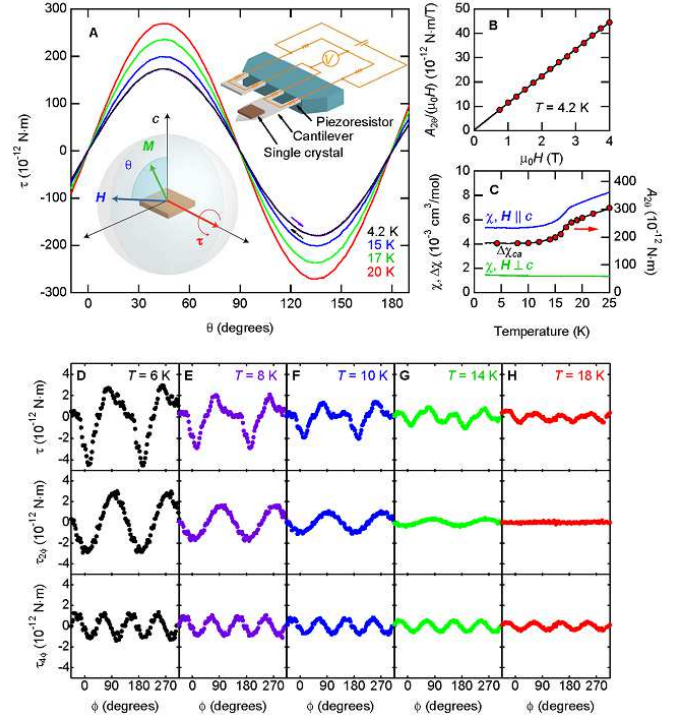


FIG. 2. Magnetic torque curves measured at $|\mu_0 \mathbf{H}| = 4$ T. (A) Torque $\tau(\theta)$ as a function of the polar angle θ (lower inset) measured at several temperatures. Torque curves measured by rotating \mathbf{H} in clockwise (dotted line) and anticlockwise (solid line) directions coincide. Upper inset illustrates the experimental configuration for $\tau(\theta)$ measurements. (B) Magnetic field dependence of the amplitude of the two-fold oscillation of the torque divided by the field, $A_{2\theta}/(\mu_0 H)$, at $T = 4.2$ K. (C) Left axis: Temperature dependence of the susceptibility χ for $\mathbf{H} \perp c$ (green) and $\mathbf{H} \parallel c$ (blue). Their difference $\Delta\chi_{ca}$ is shown in black. Right axis: Temperature dependence of $A_{2\theta}$ (red circles). (D to H) Upper panels show raw torque curves $\tau(\phi)$ as a function of the azimuthal angle ϕ at several temperatures. Middle and lower panels show the two-fold $\cos 2\phi$ and four-fold $\sin 4\phi$ components of the torque curves, respectively, obtained from Fourier analysis of the raw torque curves.

rapidly with decreasing temperature in a manner quite different from $\Delta\chi_{ca}(T)$ (Fig. 2C). This indicates that a misalignment of \mathbf{H} from the ab plane is unlikely to be the origin of the two-fold symmetry. On the basis of this reasoning, we conclude that the amplitude of two-fold oscillations is a manifestation of intrinsic in-plane anisotropy of the susceptibility (Fig. 1B):

$$\chi[110] = \chi_{aa} + \chi_{ab} \neq \chi[\bar{1}10] = \chi_{aa} - \chi_{ab}. \quad (3)$$

The in-plane anisotropy that sets in precisely at T_h indicates that the rotational symmetry is broken in the hidden-order phase. The temperature dependence of $|A_{2\phi}| \propto \chi_{ab}$ near T_h is fitted with $\chi_{ab} \propto c(T_h - T) + c'(T_h - T)^2$ much better than with a purely quadratic fit (Fig. 3A, inset). The leading T -linear term near T_h

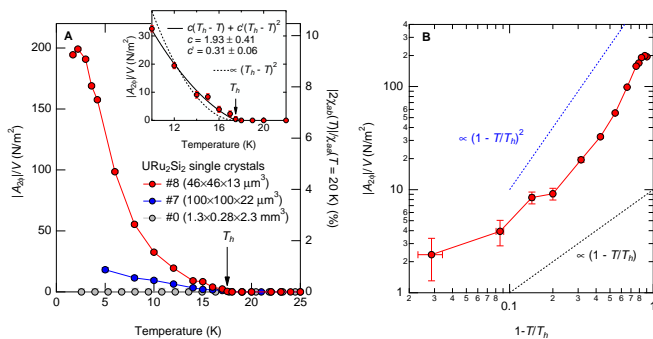


FIG. 3. (A) Temperature dependence of two-fold oscillation amplitude divided by the sample volume $|A_{2\phi}|/V$ measured for sample 7 (blue circles) and sample 8 (red circles). The normalized in-plane susceptibility anisotropy $2\chi_{ab}/\chi_{aa} = (\chi[110] - \chi[\bar{1}10])/\chi[100]$ is evaluated in the right axis. SQUID data for the large crystal, sample 0, are also shown (gray circles) in the same scale. Inset: the data for sample 8 near $T_h = 17.5$ K are fitted to $c(T_h - T) + c'(T_h - T)^2$ (solid line) and the quadratic dependence $\propto (T_h - T)^2$ (dashed line). (B) Temperature variation of $|A_{2\phi}|/V$ for sample 8 on a log-log scale. The black and blue dotted lines represent linear and quadratic temperature dependence, respectively.

(Fig. 3B) is naturally expected from the standard Landau theory of second-order transition when χ_{ab} is described by the squared term of an order parameter $\eta \propto (T_h - T)^{1/2}$. Thus, the observed in-plane anisotropy $2\chi_{ab}/\chi_{aa}$ implies that the hidden-order parameter η breaks the four-fold tetragonal symmetry.

Why has such an in-plane magnetic anisotropy not been reported before? To address this, we measured several samples with different sizes. In millimeter-sized crystals, we observed no difference between $\chi[110](T)$ and $\chi[\bar{1}10](T)$, but in samples with a smaller volume V , a nonzero $2\chi_{ab} \propto |A_{2\phi}|/V$ appeared (Fig. 3A). This may imply that the hidden-order phase forms domains with different preferred directions in the ab plane, which may be a natural consequence of the tetragonal crystal structure (with possible small undetected orthorhombicity in the domain). A domain size on the order of tens of microns would explain both our results and the difficulties in observing this effect. The fact that the torque curves remain unchanged for field-cooling conditions at different field angles [22] implies that the formation of such domains is predominantly determined and strongly pinned by the underlying crystal conditions, such as internal stress or disorder.

We now comment on the relevance of the present observation to other experimental results. The nuclear magnetic resonance (NMR) spectra have been reported to exhibit an anomalous broadening in the hidden-order phase for $\mathbf{H} \parallel ab$ [5, 6, 24]. This phenomenon has been discussed in terms of the orbital currents associated with the breaking of time-reversal symmetry [20]. The present results

provide an alternative explanation to this: Finite values of χ_{ab} give rise to the broadening of the NMR spectrum, which is estimated to be ~ 1 Oe at 4 T [22], roughly the same as the reported values [6]. We also note that some of the nuclear quadrupole frequency ν_Q measurements [25], which are sensitive to the local charge density, report a small change in the slope of $\nu_Q(T)$ at the Ru site below T_h . As for the crystal structure, no discernible lattice distortions have been reported. This may be a result of the weak coupling between the lattice and electronic excitations relevant to the two-fold symmetry. The symmetry of superconductivity, which appears at $T_c = 1.4$ K and is embedded in the hidden-order phase, should also be restricted by the found rotational asymmetry. Recently, a chiral d -wave superconducting state of the form

$$\sin \frac{k_z}{2} c \left(\sin \frac{k_x + k_y}{2} a + i \sin \frac{k_x - k_y}{2} a \right) \quad (4)$$

has been proposed [10]. The rotational symmetry breaking implies that the states including $\sin \frac{k_x + k_y}{2} a$ and $\sin \frac{k_x - k_y}{2} a$ have different superconducting transition temperatures T_{c1} and $T_{c2} (< T_{c1})$, which results in a phase transition inside the superconducting phase at T_{c2} . A recently reported anomaly in the lower critical field measurements appears to support such exotic superconducting states [26].

Our results, together with the absence of a large magnetic ordered moment, impose constraints on theoretical models of the hidden order in URu_2Si_2 . The breaking of the four-fold rotational symmetry in a tetragonal crystal structure is in general a hallmark of electronic nematic phases [27]. Electronic states that break crystal rotational symmetry without showing ordered moments have also been suggested in various strongly correlated electron systems, including $\text{Sr}_3\text{Ru}_2\text{O}_7$ [28], high- T_c cuprates [29], and frustrated magnets [30], which are discussed in terms of stripe or nematic orders. Our finding of a directional electronic state in a heavy-fermion material is another example of such exotic order in correlated matter.

-
- [1] T. T. M. Palstra *et al.*, Superconducting and magnetic transitions in the heavy-Fermion system URu_2Si_2 . *Phys. Rev. Lett.* **55**, 2727-2730 (1985).
 - [2] M. B. Maple *et al.*, Partially gapped Fermi surface in the heavy-electron superconductor URu_2Si_2 . *Phys. Rev. Lett.* **56**, 185-188 (1986).
 - [3] A. P. Ramirez *et al.*, Nonlinear susceptibility as a probe of tensor spin order in URu_2Si_2 . *Phys. Rev. Lett.* **68**, 2680-2683 (1992).
 - [4] C. Broholm *et al.*, Magnetic excitations and ordering in the heavy-electron superconductor URu_2Si_2 . *Phys. Rev. Lett.* **58**, 1467-1470 (1987).
 - [5] K. Matsuda, Y. Kohori, T. Kohara, K. Kuwahara, H.

- Amitsuka, Spatially inhomogeneous development of antiferromagnetism in URu₂Si₂: evidence from ²⁹Si NMR under pressure. *Phys. Rev. Lett.* **87**, 087203 (2001).
- [6] S. Takagi *et al.*, No evidence for “small-moment antiferromagnetism” under ambient pressure in URu₂Si₂: single-crystal ²⁹Si NMR study. *J. Phys. Soc. Jpn.* **76**, 033708 (2007).
- [7] H. Amitsuka *et al.*, Pressure-temperature phase diagram of the heavy-electron superconductor URu₂Si₂. *J. Magn. Mater.* **310**, 214-220 (2007).
- [8] J. Schoenes, C. Schönenberger, J. J. M. Franse, A. A. Menovsky, Hall-effect and resistivity study of the heavy-Fermion system URu₂Si₂. *Phys. Rev. B* **35**, 5375-5378 (1987).
- [9] K. Behnia *et al.*, Thermal transport in the hidden-order state of URu₂Si₂. *Phys. Rev. Lett.* **94**, 156405 (2005).
- [10] Y. Kasahara *et al.*, Exotic superconducting properties in the electron-hole-compensated heavy-Fermion “semimetal” URu₂Si₂. *Phys. Rev. Lett.* **99**, 116402 (2007).
- [11] C. R. Wiebe *et al.*, Gapped itinerant spin excitations account for missing entropy in the hidden-order state of URu₂Si₂. *Nature Phys.* **3**, 96-99 (2007).
- [12] P. Santini, G. Amoretti, Crystal field model of the magnetic properties of URu₂Si₂. *Phys. Rev. Lett.* **73**, 1027-1030 (1994).
- [13] A. Kiss, P. Fazekas, Group theory and octupolar order in URu₂Si₂. *Phys. Rev. B* **71**, 054415 (2005).
- [14] K. Haule, G. Kotliar, Arrested Kondo effect and hidden order in URu₂Si₂. *Nature Phys.* **5**, 796-799 (2009).
- [15] F. Cricchio, F. Bultmark, O. Grånäs, L. Nordström, Itinerant magnetic multipole moments of rank five as the hidden order in URu₂Si₂. *Phys. Rev. Lett.* **103**, 107202 (2009).
- [16] H. Harima, K. Miyake, J. Flouquet, Why the hidden order in URu₂Si₂ is still hidden—one simple answer. *J. Phys. Soc. Jpn.* **79**, 033705 (2010).
- [17] H. Ikeda, Y. Ohashi, Theory of unconventional spin density wave: a possible mechanism of the micromagnetism in U-based heavy Fermion compounds. *Phys. Rev. Lett.* **81**, 3723-3726 (1998).
- [18] V. P. Mineev, M. E. Zhitomirsky, Interplay between spin-density wave and induced local moments in URu₂Si₂. *Phys. Rev. B* **72**, 014432 (2005).
- [19] S. Elgazzar, J. Ruzs, M. Amft, P. M. Oppeneer, J. A. Mydosh, Hidden order in URu₂Si₂ originates from Fermi surface gapping induced by dynamic symmetry breaking. *Nature Mater.* **8**, 337-341 (2009).
- [20] P. Chandra, P. Coleman, J. A. Mydosh, V. Tripathi, Hidden orbital order in the heavy Fermion metal URu₂Si₂. *Nature* **417**, 831-834 (2002).
- [21] C. M. Varma, L. Zhu, Helicity order: Hidden order parameter in URu₂Si₂. *Phys. Rev. Lett.* **96**, 036405 (2006).
- [22] See supporting material on *Science* Online.
- [23] A. del Moral, J. I. Arnaud, J. S. Cockaday, E. W. Lee, Magnetic anisotropy in the paramagnetic phase of TbAl₂. *J. Magn. Mater.* **40**, 331-338 (1984).
- [24] O. O. Bernal *et al.*, ²⁹Si NMR and hidden order in URu₂Si₂. *Phys. Rev. Lett.* **87**, 196402 (2001).
- [25] O. O. Bernal *et al.*, Hidden order and disorder effects in URu₂Si₂. *Physica B* **378-380**, 574-575 (2006).
- [26] R. Okazaki *et al.*, Anomalous temperature dependence of lower critical field in ultraclean URu₂Si₂. *J. Phys. Soc. Jpn.* **79**, 084705 (2010).
- [27] E. Fradkin, S. A. Kivelson, M. J. Lawler, J. P. Eisenstein, A. P. Mackenzie, Nematic Fermi fluids in condensed matter physics. *Annu. Rev. Condens. Matter Phys.* **1**, 153-178 (2010).
- [28] R. A. Borzi *et al.*, Formation of a nematic fluid at high fields in Sr₃Ru₂O₇. *Science* **315**, 214-217 (2007).
- [29] M. Vojta, Lattice-symmetry breaking in cuprate superconductors: stripes, nematics and superconductivity. *Adv. Phys.* **58**, 699-820 (2009).
- [30] N. Shannon, T. Momoi, P. Sindzingre, Nematic order in square lattice frustrated ferromagnets. *Phys. Rev. Lett.* **96**, 027213 (2006).
- [31] We thank D. F. Agterberg, A. V. Balatsky, A. Buzudin, H. Harima, R. Ikeda, K. Ishida, Y. Kohori, T. Sakakibara, A. Schofield, H. Shishido, M. Sgrist, T. Takimoto, A. Tanaka, P. Thalmeier, and Y. Yanase for helpful discussions. Supported by Grant-in-Aid for the Global COE program “The Next Generation of Physics, Spun from Universality and Emergence”, Grant-in-Aid for Scientific Research on Innovative Areas “Heavy Electrons” (20102002, 20102006) from the Ministry of Education, Culture, Sports, Science & Technology, and Grant-in-Aid for Scientific Research from the Japan Society for the Promotion of Science.